

Increasing Specific Capacitance by Optimization of the Thickness of Carbon Electrodes

Veronika Zahorodna,^[a, b] Denys S. Butenko,^[a] Iryna Roslyk,^[a, c] Ivan Baginskyi,^[a] Volodymyr Izotov,^[a] and Oleksiy Gogotsi^{*[a, b]}

Increasing energy density without sacrificing the lifetime, power and cyclability of electrochemical capacitors is a very important goal. However, most efforts are directed toward the improvement of active charge-storing materials, while the design of devices and minimization of the weight/volume of the passive component have received less attention. We propose here a mathematical model of a carbon supercapacitor in organic electrolyte, which establishes a relationship between the specific capacitance of a device, the thickness of its electrodes, and the weight of its passive components (case, external

current leads, current collectors, etc.). The model was built based on experimentally obtained dependences and has been validated using experiments with electrodes made of two porous carbon materials. Regardless of the pore size distribution in the specified range of electrode thicknesses, the functional dependence of the electrode's specific capacitance on the thickness is well described within the linear approximation. The developed model enables optimization of the electrode thickness, thus maximizing specific energy density for a chosen carbon electrode material.

Introduction

Supercapacitors (SCs) or electrical double-layer capacitors have several advantages over other rechargeable energy sources.^[1,2] Their specific power reaches 15 kW/kg, the operating temperature range of SCs with carbon electrodes and an organic electrolyte varies from -40°C to $+80^{\circ}\text{C}$, and charge/discharge cycles during which the SC parameters remain unchanged reach at least 100,000. They are widely used in the automotive, electronic, and renewable energy industries.^[3] However, alongside the above advantages, SCs have a significant weakness that limits their practical application – a relatively low energy density.^[4] It should be noted that a wide field of SCs applications exists where high power is not required, but high energy density is needed. For example, SCs with high specific capacitance are in demand in electronics and portable devices.^[5,6] Therefore, searching for ways to increase the energy density of the SCs is one of the most topical challenges researchers face. This problem is being solved in two main directions – the application of new porous materials with a high specific capacitance and the development of new design solutions for SCs.

Nowadays, porous carbon materials, obtained from biomass (coconut shells, charcoal, or peat) by chemical or physical activation in the $800\text{--}900^{\circ}\text{C}$ temperature range^[7] are widely used in commercial SCs. The advantage of biomass-derived

porous carbon materials is their low cost. However, they have a significant drawback – a wide scattering of pore size distribution,^[8] significantly affecting the specific parameters of SCs, especially their capacitance.

Porous carbon materials derived from metal carbides (Carbide Derived Carbons, CDCs) are much more promising for achieving higher capacitance. CDCs are typically synthesized by chemical etching of metal carbides (TiC, SiC, Mo_2C , B_4C , etc.) with chlorine gas at temperatures from 200°C to 1200°C . These nanoporous carbons have a high specific surface area ($1000\text{--}2000 \text{ m}^2/\text{g}$) and, what is very important, tunable almost monodisperse pore sizes.^[9–11] The pore diameter in TiC-CDC usually varies from 5 \AA to 11 \AA , which enables the selection of the material in accordance by matching the size of solvated electrolyte ions. They also have a higher density than activated carbon, offering a higher volumetric capacitance, and a higher conductivity, allowing for the use of thicker electrodes. In addition, the thermal and electrochemical stability of CDCs in both aqueous and organic electrolytes makes them a promising alternative to biomass-derived carbon materials.^[10]

Economically, the CDC synthesis process remains relatively expensive, and it cannot compete in price with activated carbon materials obtained from biomass to produce high-power SCs. However, using CDC for the SCs fabrication with a high energy density is promising. Currently porous carbon material makes up 20–30% of the total weight of SC.^[12] The low content of porous carbon material in SC is a significant factor determining its low energy density. Denser and more conductive carbons are expected to enhance the SC-specific capacitance by increasing electrode thickness.^[13,14] As shown in ref.,^[15] coarse carbon powders can be used for electrodes with a thickness of more than $250 \mu\text{m}$. This leads to an increase in the content of the active material in the electrodes and a significant reduction in the cost of SC electrode manufacturing by eliminating the grinding stage in material processing. Previous studies have

[a] V. Zahorodna, D. S. Butenko, I. Roslyk, I. Baginskyi, V. Izotov, O. Gogotsi
Materials Research Center, 3 Krzhizhanovskogo str, 03142 Kyiv, Ukraine
E-mail: agogotsi@mrc.org.ua

[b] V. Zahorodna, O. Gogotsi
Y-Carbon Ltd, 18, Vasylevskoi str, 04116 Kyiv, Ukraine

[c] I. Roslyk
Ukrainian State University of Science and Technologies, 4, Gagarina Avenue,
49600 Dnipro, Ukraine

shown the prospects for developing of SCs with a high specific capacitance based on electrodes with a thickness of more than 200 μm , even reaching a millimeter.^[15] However, the lack of a mathematical model that establishes a relationship between the SC-specific capacitance, electrode thickness, and the passive components of the SC, retards further design and use of SCs with thick electrodes and performance exceeding the current state-of-the-art devices.

The purpose of this work is to develop of a mathematical model for SC to establish a relationship between the specific capacitance of the SC, electrode thickness and weight of its passive components (case, external current contacts, current collectors, etc.).^[16,17] The development of a mathematical model is based on the analysis of obtained experimental data for the dependence of the electrode's specific capacitance on thickness. Experimental data were obtained for electrodes fabricated using two carbon materials with significantly different pore size distributions. The first series of experiments was carried out on electrodes made of TiC-CDC, nanostructured microporous carbon derived from technical abrasive titanium carbide, and the second series was carried out on the electrodes made of the commercially available activated carbon Kuraray YP-50F (Kuraray Noritake, (Japan)).^[18] The electrodes' thickness in both series of experiments varied from 200–800 μm . From a fundamental viewpoint, the results indicate that, regardless of the pore size distribution in the specified range of electrode thicknesses, the functional dependence of the electrode's specific capacitance on the electrode thickness is well described within the linear approximation. This statement became a basis for the mathematical model proposed in this work. Within the framework of the proposed model, the equation that determines the electrode thickness, providing the maximum specific energy density of the SC depending on the design of the SC, was obtained. The optimal electrode thickness was calculated for the SC with a capacitance of 460 F, manufactured in a soft case with the shape of a parallelepiped. The fabricated SC sample is in good agreement with the model calculations. In practice, the obtained results can be used to determine the optimal electrode thickness in various designs of SC with a high energy density.

Experimental Methods

Materials

Two types of porous carbon materials were used in this research: a commercially available activated porous carbon powder Kuraray YP-50F (YP-50F) produced at an industrial scale by Kuraray Noritake (Japan) – information about its properties is presented on the company's website,^[18] and microporous nanostructured CDC powder obtained from titanium carbide. It was experimentally synthesized at the lab scale by Carbon-Ukraine (Y-Carbon Ltd., Kyiv, Ukraine). A procedure for chlorination of titanium carbide and TiC-CDC synthesis has been described previously,^[19] where we presented the main steps of the procedure for obtaining CDC powder. In the first stage, the TiC powder is granulated with polyvinyl acetate and loaded into a quartz boat. Next, the boat is placed in a tube furnace and heated to 800 °C under Argon flow

(198 ml/min). Then a flow of Cl₂ (370 ml/min) is passed through the furnace at 800 °C for 6.5 hours. Next, a stream of H₂ (492 ml/min) is passed through the furnace at 600 °C for 2 hours. When the CDC synthesis process has been completed, the furnace is cooled down in an Argon flow.

Material Characterization

The particle size distribution of the powders was measured using FEI Magellan 400 XHR (Aladdin Industrial Co.). The pore size distribution was calculated on nitrogen adsorption and desorption isotherms at a temperature of -196 °C. The measurements were carried out on ASAP 2020, Micrometrics instrument at a relative pressure ranging from 10⁻⁵ to 1. The Renishaw inVia Spectrometer (Renishaw Instruments, Gloucestershire, UK) and a 633 nm HeeNe laser were used to measure the Raman spectroscopy. Pore size distribution was calculated using the non-local density functional method (NL-DFT) which was used in the software V4.01 (B4.B 01 J), attached to the ASAP 2020 instrument. Raman micro spectroscopy (DFS-52, Ar laser, 514 nm) was used to study the material composition.

Manufacturing of Electrodes

Current collectors of the electrodes were made of 20 μm thick aluminum foil. To reduce the contact resistance between the current collector and a carbon-containing component of the electrodes, the current collectors were processed according to the electro-spark alloying method.^[20] The current collector is connected to the carbon-containing component of the electrodes by an adhesive film formed on its surface. The adhesive film with a thickness of 10 μm was applied in a suspension form to the surface of the current collector using a "doctor blade" device. Applied suspension consisted of polytetrafluoroethylene (PTFE) 1.29 wt %, conductive Super-P carbon black (Nippon) in N-methyl-2-pyrrolidone 96.78 wt %. (NMP, Sigma Aldrich). Next, the collector was placed in a vacuum-drying oven for three hours at a temperature 120 °C. After drying, the thickness of the adhesive layer was 3 μm .

The carbon-containing component of YP-50F and CDC-based electrodes were fabricated using a mixture that included porous carbon (91 wt %), PTFE binder from Sigma Aldrich (6 wt %), and conductive carbon black Super-P (3 wt %). All these components were added to an aqueous solution of 20% alcohol and thoroughly mixed into paste in an agate mortar. After that, carbon-containing electrode films (carbon electrodes) with thicknesses of 200, 400, 600, and 800 μm were produced by the rolling method.^[21] The thickness of carbon electrodes made of both, CDC and YP-50F powders, was the same. Next, the carbon film was pressed to the current collector and placed in a vacuum-drying oven for 1 hour at 170 °C. Then the electrodes were rolled with a roller heated to 180 °C. The size of all produced electrode samples was 20 mm * 20 mm. In the last stage, the electrodes were placed in a vacuum-drying oven at a temperature of 150 °C for 24 hours before device assembly.

Manufacturing of SC Prototypes

SC prototypes were assembled in a sealed glove box. The water content inside the glove box was <0.01 ppm, and the oxygen content was <0.01 ppm. During assembly, the SC electrodes were separated by a Nippon Kodoshi Corporation TF48-40 separator with a 40 μm thickness. The SC case was made of a 130 μm film (DNP1-40 h) (Dai Nippon Printing Corporation, Ltd.). 1.3 M solution of

triethyl-methylammonium tetrafluoroborate salt (TEMABF₄) in acetonitrile (Sigma Aldrich) was used as an electrolyte.

Electrochemical Measurements

The IviumStat instrument (Ivium Technologies, Eindhoven, Netherlands) and ARBIN BT2000 (E) battery tester (Arbin Instruments, USA) were used for electrochemical measurements. Galvanostatic charge (GC) measurements were carried out to determine the specific current density, which varied from 0.1 A/g to 1 A/g. Electrochemical impedance spectroscopy (EIS) measurements were carried out in the frequency range from 0.01 Hz to 100 kHz. Cyclic voltammetry (CV) measurements were conducted at sweep rates from 1 mV/s to 1000 mV/s. The specific gravimetric capacitance of carbon powders (c_g , F/g) was calculated for the mass of material contained in two electrodes based on the discharge CV curves by the following equation:

$$c_g = \frac{1}{2 \cdot m_{act} \cdot v \cdot t} \int_0^t i(\tau) d\tau$$

where t – discharge time, $i(\tau)$ – the dependence of the charge (discharge) current on time, m_{act} – the mass of the active material (carbon) in one electrode, v – potential sweep rate.

Results and Discussion

TiC-CDC powder was used to manufacture electrode material without grinding and sieving. As a result, the particles from 80–150 µm were present in the CDC electrode. The packing density of CDC and YP-50F in the electrodes was 0.56 g/cm³ and 0.53 g/cm³, respectively.

The microstructure of CDC powder was analyzed by a field emission scanning electron microscope (FE-SEM Magellan 400) and is shown in Figure 1a and b. Measurements of Raman spectroscopy were performed with a 633 nm HeeNe laser and a Renishaw inVia Spectrometer (Renishaw Instruments, Gloucestershire, UK); typical D and G bands were observed in the CDC and YP-50F powders (Figure 1c), that indicate the presence of highly disordered graphitic carbon. The nature of the CDC pores and porosity were determined by analysing of the nitrogen adsorption/desorption isotherms. The measurements were carried out at a temperature of −176 °C, with a relative relative pressure change of the from 10^{−5} to 1. Typical adsorption/desorption isotherms for CDC are shown in Figure 1d. They are close to Type I, with a tiny uplift at a relative pressure above 0.9, which makes us classify it at Type IV. Saturation is observed on the adsorption isotherm at a relative pressure of 0.1. This indicates that micropores and pores smaller than 2 nm dominate in this CDC. The absence of mesopores in the material is indicated by the non-inversion of the adsorption/desorption isotherms at a relative pressure of 0.9. The specific surface area

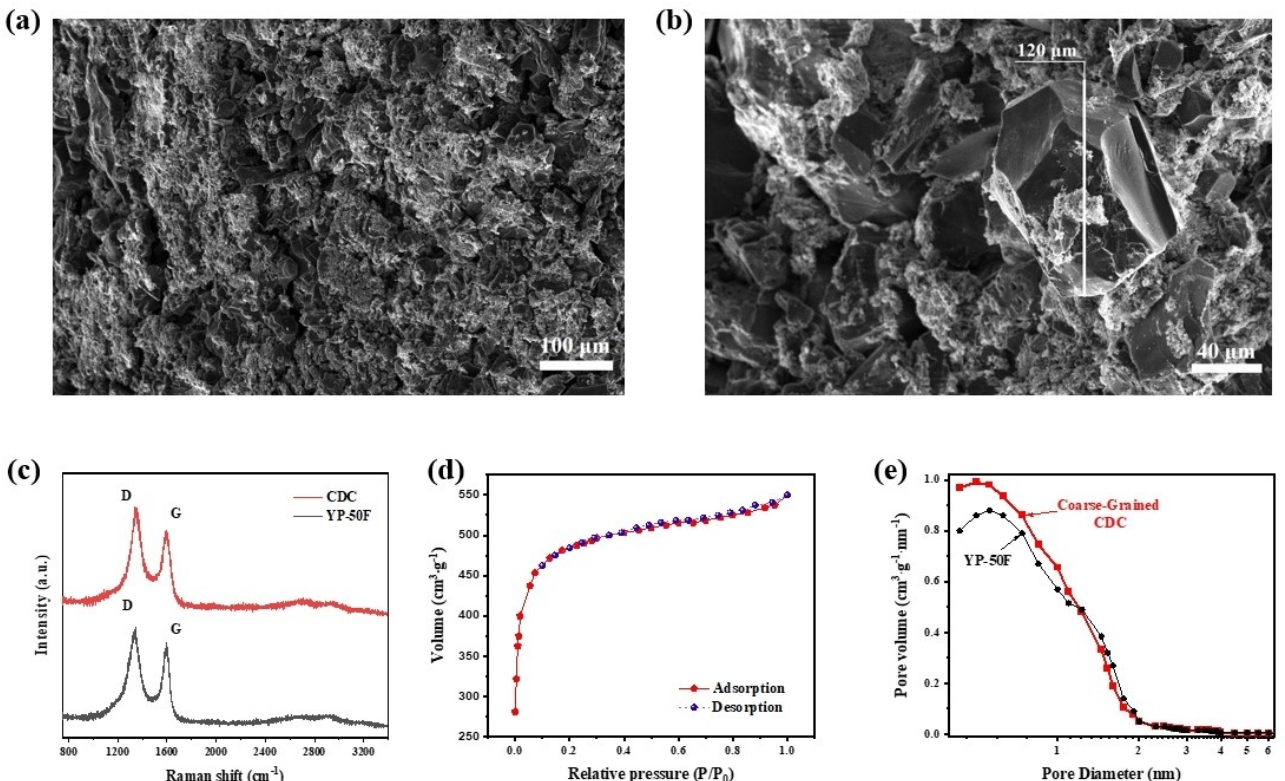


Figure 1. Characterization of the materials: TiC-CDC: SEM image of the TiC-CDC (a-b), Raman spectrum for TiC-CDC and reference data for YP-50F (c), TiC-CDC adsorption and desorption isotherms of nitrogen molecules (d), and pore size distribution for TiC-CDC and reference data on pore size distribution for YP-50F (e).

and the pore size distribution (Figure 1e) were calculated by two-dimensional non-local density functional theory (NLDFT), which assumes the slit nature of the pores.^[22] The calculated specific pore surface area is 1440 m²/g. Figure 1e compares reference pore size distribution data for YP-50F carbon powder. It should be noted that the surface area of carbon powders was reduced after mixing with a PTFE binder because the binder blocks entries to some pores.^[23]

The dependence of the specific capacitance of CDC powders and YP-50F on the thickness of carbon-containing films was studied for the films with a thickness of 200, 400, 600, and 800 μm. The films were deposited on 20 μm thick aluminum current collectors. Fabricated electrodes were studied in a two-electrode symmetrical prototypes of supercapacitors. SC electrodes were separated by a 40 μm thick DNPel-40 h separator. A 1.3 M solution of TMEABF₄/ACN solution was used as the electrolyte.

Galvanostatic measurements of the charge and discharge of SC prototypes were carried out at a current density ranging from 0.1 A g⁻¹ to 1 A g⁻¹ and a voltage range from 0 to 2.7 V. The results of measurements for a current density of 0.5 A g⁻¹ are shown in Figure 2a and c. The triangular shape of charge/discharge curves shown in the figures indicates the electrostatic double-layer mechanism of the electrochemical processes occurring in the SC. As seen in Figure 2a and c, the charging/discharging time for the SC prototypes decreases with increasing carbon layer thickness. This indicates a decrease in the specific capacitance of carbon powder contained in the film. The increasing IR drop (electrode resistance) with increasing thickness was also observed. Figure 2a and c also show that the

specific capacitance of carbon electrodes decreases with increasing current density during the cycling of SC.

Figure 2b and d show the Nyquist plots obtained for SC prototypes in the frequency range from 0.01 Hz to 100 kHz. In a low-frequency region, the graph curves have almost vertical lines for all devices. This means that the only processes that is associated with the charge is the electric double-layer formation in all SCs.^[24,25] The shape of the curves in a high-frequency region shows a low value of the equivalent series resistance (ESR) of SC prototypes and a low contact resistance between the aluminum current collectors and carbon-containing films. Low contact resistance is provided due to the modification of the aluminum current collector by electro-spark treatment.^[20] There is a Warburg element in the mid-frequency region of the spectra. The length of the Warburg region increases with the thickness of the carbon electrode. This indicates that the diffusion distance increases when the film thickness is larger, which leads to an increase in ionic resistance.

Figure 3a and c show the results of cyclic voltammetry at a potential sweep rate of 20 mV/s. Calculations of the specific gravimetric capacitance were carried out considering the mass of carbon powder contained in two electrodes. Based on the experimental data on the specific gravimetric capacitance and concentration of carbon powder in the electrode film, the specific volumetric capacitances of the carbon electrodes and electrochemical capacitor as a whole were calculated. Figure 3b and e show the dependences of the carbon electrode's specific volumetric capacitance as a function of the film thickness. Figure 3b and d show that with increasing film thickness, the specific capacitance is reduced. Such dependency on the

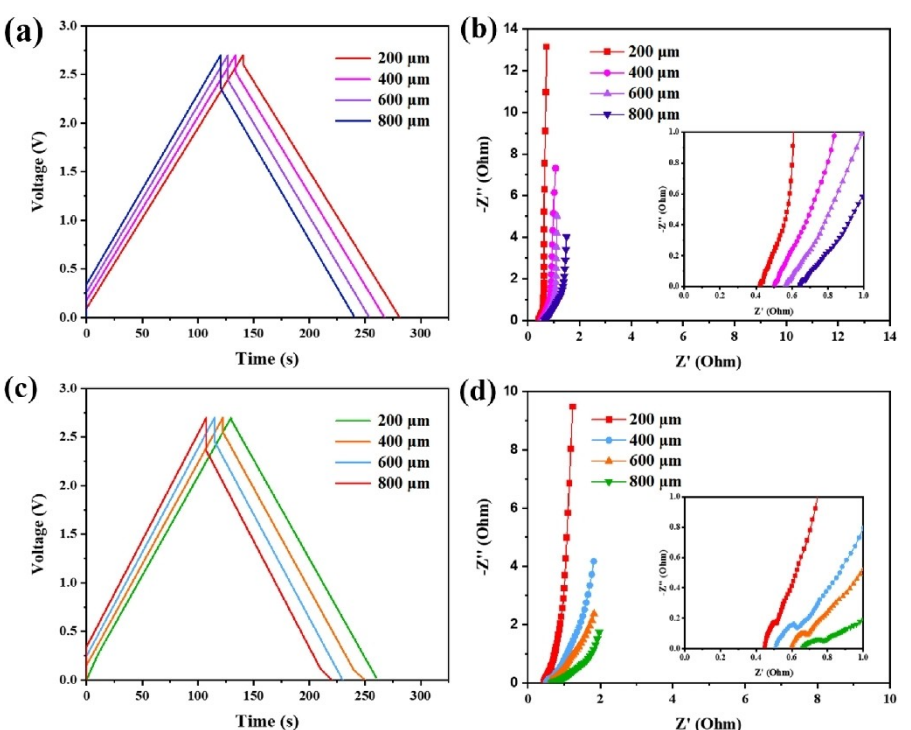


Figure 2. Galvanostatic charge/discharge curves at a current density of 0.5 A g⁻¹ for supercapacitors made of CDC (a) and YP-50F (c); Nyquist plots for CDC (b) and YP-50F (d) based supercapacitors.

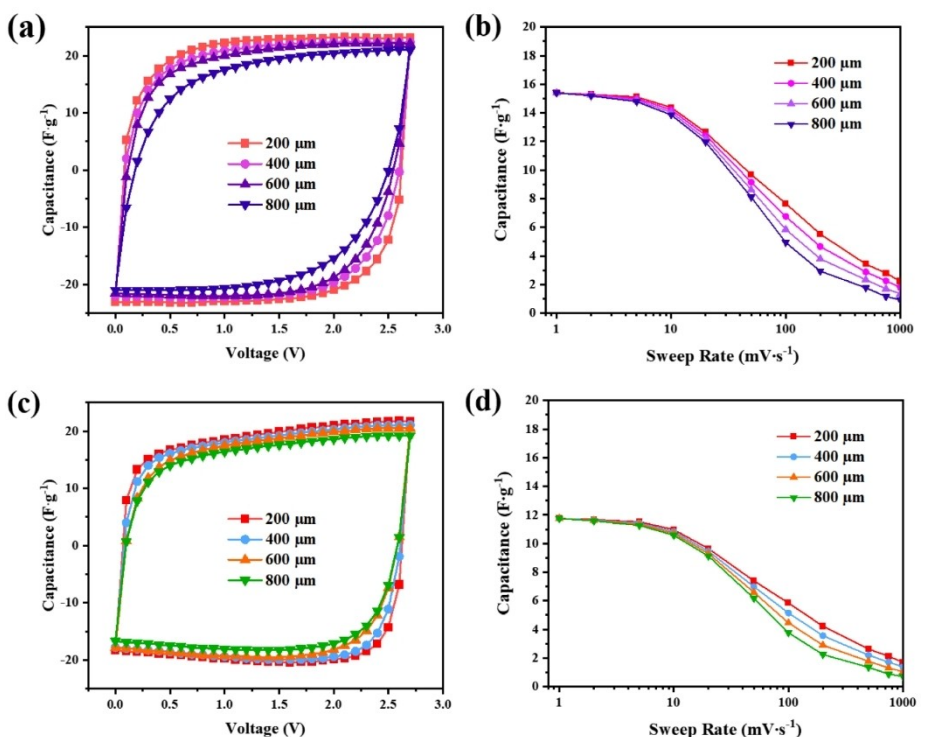


Figure 3. Cyclic voltammograms for supercapacitors with different thicknesses of carbon electrode films made of (a) CDC and (c) YP-50F powders at a sweep rate 20 mV/s⁻¹; dependences of the specific volumetric capacitance of carbon electrode films made of CDC (b) and YP-50F (d) powders on the sweep rate.

specific capacitance is explained by diffusion limitations caused by the movement of electrolyte ions in the films. Diffusion limitations lead to insufficient time for full charging during a sweep and, as a result, the thicker the carbon electrode is, the larger part of it remains incompletely charged.^[25]

Besides active components (carbon electrodes) and electrolytes, the electrochemical supercapacitors contain passive elements, such as metal current collectors and a separator. The content of carbon powder in SC is defined as the ratio of carbon powder mass per total volume of the SC (the sum of the volumes of carbon electrode films and passive elements). The contents of carbon powders in SC for different thicknesses of carbon films are shown in Table 1.

The specific capacitance of the SC reflects its ability to store energy. The specific capacitance of SC, as well as the specific capacitance of carbon powder, depends on the potential sweep rate. The specific capacitance of a SC for a given sweep rate was calculated as a multiplication of carbon powder concentration and its specific capacitance. Figure 4a and c show the depend-

ences of specific capacitances of the SC and on the thickness of the carbon electrode at a potential sweep rate of 10 mV/s⁻¹. The graphs on these figures show that the specific capacitance of SC increases with the increase of the film thickness. In contrast, the specific capacitance of carbon electrode has the opposite trend. This is explained by the higher concentration of carbon powder in SC with thicker films. The specific capacitance of SC is determined by two factors. The first is a concentration of carbon powder, which does not depend on the potential sweep rate and grows with increasing film thickness in SC. The second is the specific capacitance of the powder, which reduces in both cases – when the thickness of carbon-containing films or a sweep rate increases. Moreover, the thicker the film, the faster powder's specific capacitance reduces with increasing sweep rate. Figure 4b and d show the dependence of the SC specific capacitance on carbon electrode thicknesses and potential sweep rate. These figures show that for sweep rates less than 100 mV/s⁻¹, the SCs based on the films thicker than 200 μm, have a higher specific capacitance than SCs with a film

Table 1. The content of active material (carbon) in the electrochemical devices depends on the thickness of the carbon electrode films.

Carbon powder	Thickness of the carbon electrode film (μm)			
	q200	400	600	800
Content of carbon powder in the electrochemical device (g/cm ³)				
CDC	0.487	0.52	0.533	0.54
YP-50F	0.461	0.493	0.505	0.511

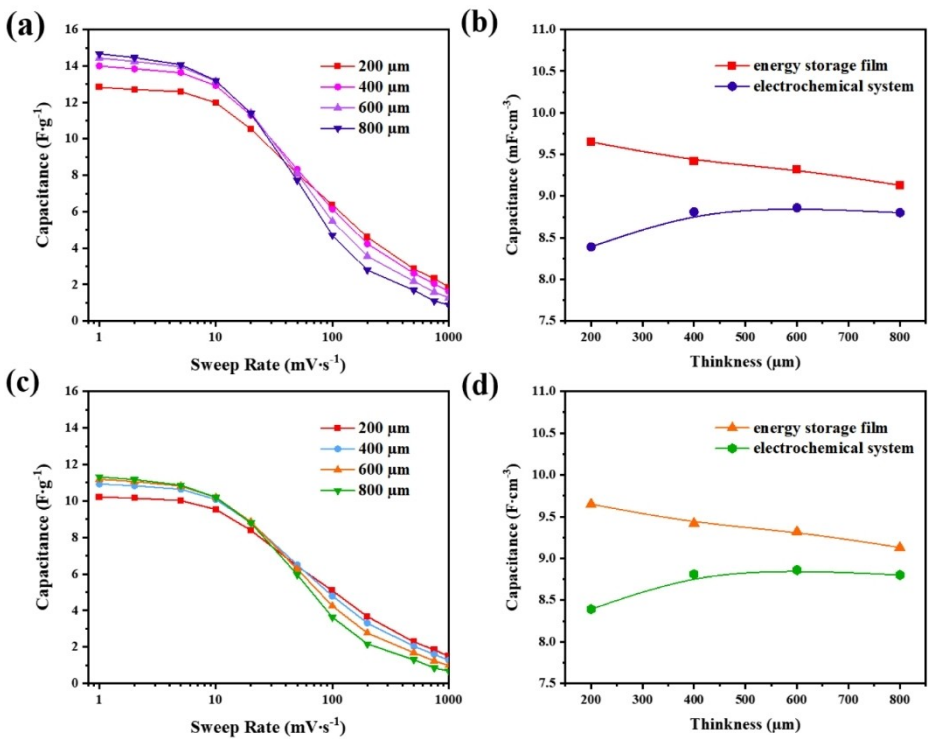


Figure 4. Dependences of SC specific capacitance and specific capacitance of based carbon electrodes made of CDC (a) and YP-50F (c) –on carbon electrode thickness at sweep rate $10 \text{ mV} \cdot \text{s}^{-1}$; dependences of SCs specific volumetric capacitance with different thicknesses of carbon electrodes made of CDC (b) and YP-50F (d) on the sweep rate.

thickness equal to $200 \mu m$ film. At s rates of more than $100 \text{ mV}/\text{s}^{-1}$, the specific capacitance of SC with $200 \mu m$ film thickness prevails over SC with thicker films.

The above calculations show that the passive elements of SCs significantly affect the dependence of the SC's specific energy density on the carbon electrode thickness. Further analysis of the experimental data allows to determine the CFF thickness that result in the SC's maximum specific capacitance.

Passive elements of the SC also significantly affect its specific capacitance. However, the effect of passive elements on the specific capacitance of the SC is challenging to determine. Therefore, the proposed mathematical model allows us to consider the effect of passive elements on the specific capacitance of the SC and calculate the carbon electrode thickness that provides the maximum specific capacitance of the SC. Such model calculations will enable manufacturing SCs with maximum specific energy density for a chosen carbon material.

Supercapacitor Model with High Specific Capacitance

Summarizing the experimental results, we can conclude that the specific capacitance of carbon material is reduced when the charge/discharge current density is increased. At the same current density values, the specific capacitance of carbon material is lower in thicker carbon electrodes.

To develop our model, we made the following assumption: at the same current density, when the carbon electrode thickness varies from h_0 to h_m , the specific gravimetric capacitance of the carbon electrode decreases linearly with increasing thickness. This assumption is based on the experimental data obtained above. Mathematically, this dependence can be described by the following equation:

$$c_g(i_0, h) = c_g(i_0, h_0) \cdot (1 - \alpha(i_0) \cdot (h - h_0)) \quad (1)$$

$$\alpha(i_0) = \frac{c_g(i_0, h_0) - c_g(i_0, h_m)}{c_g(i_0, h_0) \cdot (h_m - h_0)}$$

where $c_g(i_0, h)$ – specific gravimetric capacitance of carbon for film thickness h and current density i_0 . Using the model assumption (1), the equation describing the dependence of the SC-specific gravimetric capacitance ($C_g^{SC}(i_0, h)$) on the carbon electrode thickness, can be presented as follows:

$$C_g^{SC}(i_0, h) = \frac{\rho_{am} \cdot c_g(i_0) \cdot (1 - \alpha(i_0) \cdot h) \cdot h}{2 \cdot h \cdot (\rho_{am}^{el} + P/V) + h_{al} \cdot (P/V) + h_{sep} \cdot (\rho_{sep} + P/V)} \quad (2)$$

where h_{al} and ρ_{al} – thickness and specific density of metal current collector, h_{sep} and ρ_{sep} – thickness and specific density of separator soaked in electrolyte, ρ_{am} – specific density of carbon powder in carbon electrode, ρ_{am}^{el} – specific density of carbon electrode soaked in electrolyte, P – total weight of internal

connections, external current contacts and casing of SC, V – volume of SC device.

We have investigated $C_g^{SC}(i_0, h)$ as a variable function of h for extreme values and found expression describing the optimal thickness of carbon electrode resulted in the highest values of specific gravimetric capacitance. After simple mathematical calculations, we obtained an equation that relates the specific weight characteristics of the materials used for SC fabrication with the optimal carbon electrode thickness. The carbon electrode thickness, for maximum function $C_g^{SC}(i_0, h)$, is calculated by the equation:

$$h_e = Y \left(\sqrt{1 + \frac{1}{Y} h_0 + \frac{1}{Y \cdot \alpha(i_0)} - 1} \right); \quad (3)$$

$$Y = \frac{h_{Al} \cdot (\rho_{Al} + P/V) + h_s \cdot (\rho_s + P/V)}{2 \cdot (\rho_{am}^{el} + P/V)}$$

To validate the assumption used for the proposed mathematical model, SC prototypes were fabricated based on two different porous carbons, YP-50F and CDC, considering the optimal carbon electrode thickness. For comparison, a SC prototype carbon electrode thickness of 100 μm was fabricated using YP-50F carbon material. Indicated carbon electrode thickness was chosen considering that the maximum specific capacitance of carbon material is observed at this thickness value.^[16] Regardless of the carbon electrode thickness and carbon material selected, the volume of SC was the same in all three SC mats – 36 cm^3 . In the SC prototype based on YP-50F carbon, the concentration of activated carbon powder was the same. The SC casing was made of DNPe1-40 h film (Dai Nippon Printing Corporation, Ltd., Japan). The DNPe1-40 h film comprises aluminum foil laminated with a polypropylene film on

both sides. A photograph of the SC prototype based on the CDC is shown in Figure 5a.

Experimentally determined weight and size characteristics of the SC components were used to calculate the optimal thickness of the carbon electrode and verify the model. The coefficient was calculated by Equation (1) using experimental data obtained from cyclic voltammograms at a sweep rate of 20 mV/s^{-1} . The coefficient value for both YP-50F and CDC materials was $1.43 \times 10^{-4} \mu\text{m}^{-1}$. Aluminum foil modified by the electro-spark surface treatment was used as the current collector in the fabrication of the SC prototypes. The specific weight of the modified aluminum foil remained almost unchanged and was 2.7 g/cm^3 . The thickness of the aluminum foil was 20 μm . The separator thickness was 40 μm . The specific weight of the carbon electrode and separator, soaked in the electrolyte, was determined using the AGR-150 device and was 1.3 g/cm^3 and 1.14 g/cm^3 respectively. The average weight of SC casing with internal aluminum switching connections and external current contacts of YP-50F and CDC based SCs with optimized carbon electrode thickness was 5.6 g.

The optimal carbon electrode thickness calculated by Equation (4) was 483 μm . During the manufacturing of the SC prototype, the carbon electrode thickness was 480 μm . After manufacturing SC prototypes with optimized carbon electrode thickness, their average weight was 53.5 g. The deviation from the average weight of SC prototypes with optimized carbon electrodes thickness did not exceed 1%. The weight of the SC prototype with a carbon electrode thickness of 100 μm was 55.6 g. The increase in the weight of the SC with a CCF thickness of 100 μm is because the specific weight of its SC is higher than of the SC prototypes with a carbon electrode thickness of 480 μm . The electrical parameters for all SC prototypes regardless of the carbon electrode thickness were determined by the galvanostatic cycling method. Galvanostatic

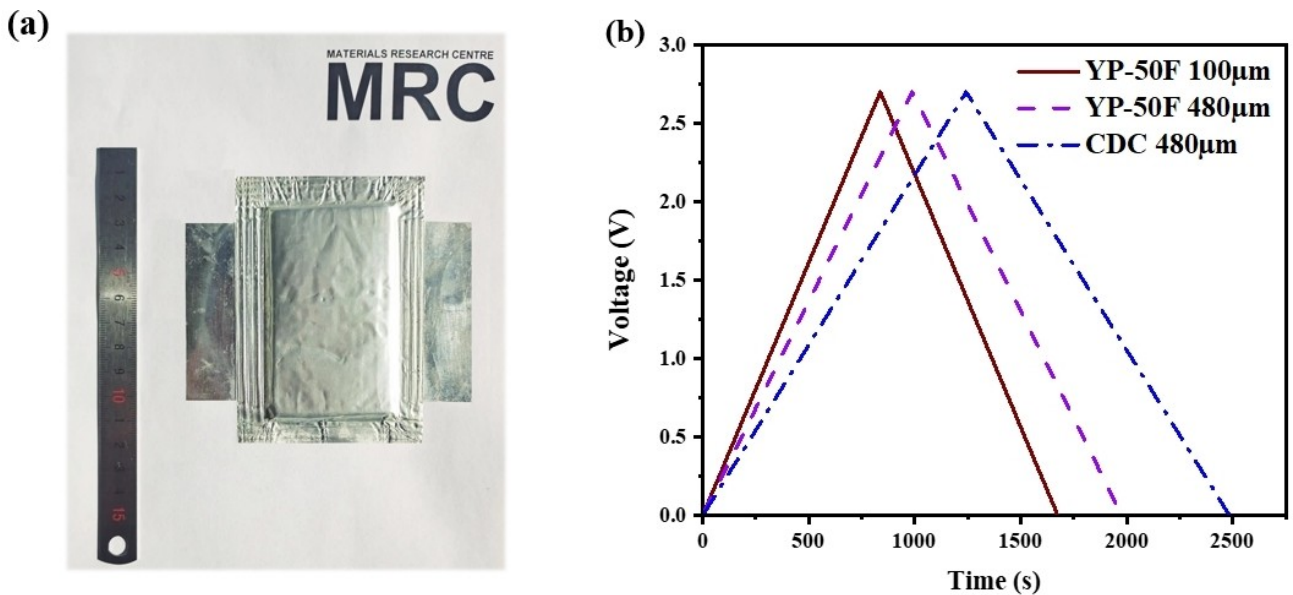


Figure 5. Prototype of a SC in a pouch cell (a); galvanostatic charge-discharge curves under current 1 A for SCs with 100 μm YP-50F-based carbon electrode (YP-50F100 μm) and 480 μm carbon electrode (YP-50F480 μm), as well as a CDC-based SC with a 480 μm carbon electrode (CDC 480 μm) (b).

cycling was carried out with a 1 A current in the voltage range from 0 to 2.7 V. The measurements were carried out on an ARBIN BT2000 (E) battery cycler and the results are shown in Figure 5b.

The capacitance of the SC, calculated considering the galvanostatic curves, for the prototypes based on YP-50F carbon was 320 F for the SC with a carbon electrode 100 µm (YP-50F100 µm) and 365 F for the SC with a carbon electrode 480 µm (YP-50F 480 µm). The energy density of the SC with 100 µm carbon electrode was 5.83 Wh/kg, and the SC with 480 µm carbon electrode was 6.91 Wh/kg, 18.5% more. These calculations show that using carbon electrode with optimized thickness for manufactured SC electrodes allows a significant increase in energy density.

The capacitance of the SC prototypes based on CDC powder with a 480 µm carbon electrode was 460 F, and its energy density was 8.71 Wh/kg. Consequently, the energy density of this SC is 49.4% higher than the energy density of the SC prototype with a 100 µm carbon electrode, made of YP-50F powder. The above experimental data and subsequent calculations show that the assumption underlying the mathematical model accurately describes the dependence of the carbon electrode's specific capacitance on its thickness.

Conclusions

We have developed a mathematical model of a carbon supercapacitor in organic electrolyte, which establishes a relationship between the specific capacitance of a device, the thickness of its electrodes, and the weight of its passive components (case, external current leads, current collectors, etc.). The mathematical model is based on the analysis of experimentally obtained dependence of the specific capacitance of carbon electrodes on their thickness. The model was validated using experiments with electrodes made of two porous carbon materials with significantly different pore size distributions. TiC-CDC had a narrower pore size distribution compared to Kuraray YP-50F activated carbon. Regardless of the pore size distribution in the specified range of electrode thicknesses, the functional dependence of the electrode's specific capacitance on the thickness is well described within the linear approximation. The developed model enables the manufacturing of SCs with the maximum specific energy density for a chosen carbon material.

Acknowledgements

This work was supported by Horizon Europe research project GREENCAP 101091572. The authors are grateful to Prof. Yury Gogotsi (Drexel University) for helpful comments on the manuscript; and Serhii Dukhnovskiy for his help with preparation of illustrative image

Conflict of Interests

The authors declare no conflict of interest.

Data Availability Statement

The data that support the findings of this study are available from the corresponding author upon reasonable request.

Keywords: Supercapacitor • specific capacitance • electrode thickness • carbon electrode • CDC

- [1] P. Simon, Y. Gogotsi, *Acc. Chem. Res.* **2012**, *46*, 1094–1103.
- [2] P. Simon, Y. Gogotsi, *Nat. Mater.* **2008**, *7*, 845.
- [3] P. Simon, Y. Gogotsi, B. Dunn, *Science (New York, N. Y.)* **2014**, *343*, 1210–1211.
- [4] F. Beguin, V. Presser, A. Balducci, E. Frackowiak, *Adv. Mater.* **2014**, *26*, 2219–2251.
- [5] M. Beidaghi, Y. Gogotsi, *Energy Environ. Sci.* **2014**, *7*, 867–884.
- [6] K. Jost, G. Dion, Y. Gogotsi, *J. Mater. Chem. A* **2014**, *2*, 10776–10787.
- [7] C. Schütter, C. Ramirez-Castro, M. Oljaca, S. Passerini, M. Winter, A. Balducci, *J. Electrochem. Soc.* **2015**, *162*, A44.
- [8] M. A. Daley, D. Tandon, J. Economy, E. J. Hippo, *Carbon* **1996**, *34*, 1191–1200.
- [9] T. Ariyanto, B. Dyatkin, G.-R. Zhang, A. Kern, Y. Gogotsi, B. J. M. Etzold, *Microporous Mesoporous Mater.* **2015**, *218*, 130–136.
- [10] V. Presser, M. Heon, Y. Gogotsi, *Adv. Funct. Mater.* **2011**, *21*, 810–833.
- [11] Y. Gogotsi, V. Presser, *Carbon Nanomaterials*, CRC Press **2013**.
- [12] J. Chmiola, G. Yushin, Y. Gogotsi, C. Portet, P. Simon, P. L. Taberna, *Science* **2006**, *313*, 1760–1763.
- [13] L. Liu, X. Wang, V. Izotov, D. Havrykov, I. Koltsov, W. Han, Y. Zozulya, O. Linyucheva, V. Zahorodna, O. Gogotsi, Y. Gogotsi, *Electrochim. Acta* **2019**, *302*, 38–44.
- [14] V. Izotov, O. Gogotsi, D. Havrykov, M. Chufarov, Y. Zozulya, O. Linyucheva, V. Zahorodna, *Optimization of Electrode Structure for Symmetric Supercapacitors with High Specific Energy Intensity, Chapter in "Promising Materials and Processes in Applied Electrochemistry"*, (Eds: V. Barsukov, Y. Borysenko, V. Khomenko, O. Linyucheva), KNUDT, Kyiv, **2018**, 22–33.
- [15] B. Dyatkin, A. Gogotsi, B. Malinovskiy, Y. Zozulya, P. Simon, Y. Gogotsi, *J. Power Sources* **2016**, *306*, 32–41.
- [16] K.-C. Tsay, L. Zhang, J. Zhang, *Electrochim. Acta* **2012**, *60*, 428–436.
- [17] A. Berrueta, A. Ursua, I. S. Martin, A. Eftekhari, P. Sanchis, *Supercapacitors: Electrical Characteristics, Modeling, Applications, and Future Trends*, IEEE Access, Vol. 7, IEEE **2019**, pp. 50869–50896.
- [18] Functional activated carbon, <https://www.kuraray.com/products/kuraray-coal>.
- [19] R. Dash, J. Chmiola, G. Yushin, Y. Gogotsi, G. Laudisio, J. Singer, J. Fischer, S. Kucheyev, *Carbon* **2006**, *44*, 2489–2497.
- [20] E. Shembel, Method of fabricating electrodes with low contact resistance for batteries and double layer capacitors, US Patent US20090130564 A1, **2009**.
- [21] J. Troop, M. Arulepp, J. Leis, A. Punning, U. Johanson, P. Viljar, A. Aabloo, *Materials* **2009**, *3*.
- [22] J. Jagiello, J. P. Olivier, *Carbon* **2013**, *55*, 70–80.
- [23] B. Xu, H. Wang, Q. Zhu, N. Sun, B. Anasori, L. Hu, F. Wang, Y. Guan, Y. Gogotsi, *Energy Storage Mater.* **2018**, *12*, 128–136.
- [24] P. Taberna, P. Simon, J. Fauvarque, *J. Electrochem. Soc.* **2003**, *150*, A292.
- [25] J. Segalini, B. Daffos, P. L. Taberna, Y. Gogotsi, P. Simon, *Electrochim. Acta* **2010**, *55*, 7489–7494.

Manuscript received: June 17, 2024

Revised manuscript received: August 29, 2024

Accepted manuscript online: September 6, 2024

Version of record online: October 31, 2024